



GLOBAL JOURNAL OF RESEARCHES IN ENGINEERING: J  
GENERAL ENGINEERING

Volume 17 Issue 3 Version 1.0 Year 2017

Type: Double Blind Peer Reviewed International Research Journal

Publisher: Global Journals Inc. (USA)

Online ISSN: 2249-4596 & Print ISSN: 0975-5861

# Performance Simulation of Two-Bed Silica Gel-Water Adsorption Chillers

By Najeh Ghilen, Souad Messai, Slimane Gabsi, Mohammed El Ganaoui  
& Riad Benelmir

*University of Lorraine France*

**Abstract-** This paper presents a transient model of a two bed silica gel - water solar adsorption cooling system. This program is then utilized to simulate the performance of a sample solar adsorption cooling system used for cooling a room that comprises an area of 9 m<sup>2</sup> located in Nancy city in France. The system has been simulated with typical weather data of solar radiation and ambient temperatures of France. The results include effects of the hot water temperature, cooling water temperature and chiller water temperature and cycle time on COP, refrigeration capacity and cycled mass are studied in order to determine their optimum values able to maximize the overall performance of the system under analysis for its adaptation to the Tunisian climate.

**Keywords:** solar adsorption chiller, silica gel-water, simulation, performance.

**GJRE-J Classification:** FOR Code: 091599



*Strictly as per the compliance and regulations of:*



© 2017. Najeh Ghilen, Souad Messai, Slimane Gabsi, Mohammed El Ganaoui & Riad Benelmir. This is a research/review paper, distributed under the terms of the Creative Commons Attribution-Noncommercial 3.0 Unported License <http://creativecommons.org/licenses/by-nc/3.0/>), permitting all non commercial use, distribution, and reproduction in any medium, provided the original work is properly cited.

# Performance Simulation of Two-Bed Silica Gel-Water Adsorption Chillers

Najeh Ghilen <sup>α</sup>, Souad Messai <sup>σ</sup>, Slimane Gabsi <sup>ρ</sup>, Mohammed El Ganaoui <sup>ω</sup> & Riad Benelmir <sup>✶</sup>

**Abstract-** This paper presents a transient model of a two bed silica gel - water solar adsorption cooling system. This program is then utilized to simulate the performance of a sample solar adsorption cooling system used for cooling a room that comprises an area of 9 m<sup>2</sup> located in Nancy city in France. The system has been simulated with typical weather data of solar radiation and ambient temperatures of France. The results include effects of the hot water temperature, cooling water temperature and chiller water temperature and cycle time on COP, refrigeration capacity and cycled mass are studied in order to determine their optimum values able to maximize the overall performance of the system under analysis for its adaptation to the Tunisian climate.

**Keywords:** solar adsorption chiller, silica gel-water, simulation, performance.

## I. INTRODUCTION

With the increasing economic development and environment protection, adsorption refrigeration technology as the green refrigeration method has received more and more attention in recent years because it can save energy and is environmentally friendly. Adsorption refrigeration can be driven by low-grade heat source, such as waste heat from the process industry and solar energy.

The adsorption cooling and heat pump systems could utilize low temperature waste heat or renewable energy sources. The working pairs of adsorption cooling and heat pump are mainly dominated by activated carbon/ammonia, activated carbon/methanol and activated carbon fiber (ACF)/ammonia, silica gel/water and zeolite/water pairs.

In this context, silica gel-water was selected as the adsorbent – adsorbate pair. Compared with other adsorbents, silica gel can be regenerated at a relatively low temperature (below 100°C, and typically about 85°C). It also has a large uptake capacity for water which has a high latent heat of evaporation; up to 40% of its dry mass. A silica gel-water adsorption chiller is able to make use of industrial waste heat to effect useful cooling.

*Author α:* Faculty of Sciences and Technology/UIT Longwy Lab. LERMAB (UdL/INRA/Labex ARBRE) University of Lorraine France, Research Unit Environment, Catalysis and Process Analysis URECAP The National School of Engineering of Gabes, Gabes, Tunisia. e-mail: najeh.ghilen@gmail.com

*Author σ ρ:* Research Unit Environment, Catalysis and Process Analysis URECAP The National School of Engineering of Gabes, Gabes, Tunisia.

*Author ω ✶:* Faculty of Sciences and Technology/UIT Longwy Lab. LERMAB (UdL/INRA/Labex ARBRE) University of Lorraine France.

Many researchers evaluated the performance of adsorption cooling and heat pump systems based on working pairs, system design and methodology. A transient simulation model for adsorption cooling system using silica gel/water pair powered by renewable energy was investigated by a number of researchers [1-7]. Restuccia et al. [8] reported an experimental and numerical study of a lab-scale adsorption chiller using the macroporous silica gel impregnated with CaCl<sub>2</sub> as the adsorbent. At a 90-95°C heat source, the authors showed that the measured COP values were up to 0.6. With the aim of improving silica gel-water adsorption chillers design with two adsorption/desorption chambers, Liu et al. [9] demonstrated that with the new chiller, a COP of about 0.5 is reached. In the same way, Núñez et al. [10] presented the development of a prototype of a small adsorption heat pump using silica gel-water pair. The purpose of minimizing primer energy consumption is achieved. In fact, for air-conditioning of 12-15°C, a cooling COP of 0.5 is found. Wang et al. [11] built and tested a novel silica gel-water adsorption chiller. For a hot water temperature of 84.8°C, a cooling water temperature of 30.6°C and a chilled water outlet temperature of 11.7°C, the measured COP is about 0.38. The authors proved that the application of this adsorption chiller is successful especially for low grade heat source. Xia et al. [12] presented an improved two bed silica gel-water adsorption chiller. The improved chiller is composed of three vacuum chambers: two adsorption/desorption vacuum chambers and one heat pipe working vacuum chamber. A heat pipe is used to combine the evaporators of the two adsorption/desorption units. An improvement of at least 12% for the COP was reached compared to the formers chillers. Hen et al. [13] investigated an improved compact silica gel-water adsorption chiller without vacuum valves. To improve the performance of the chiller, a heat and mass recovery process is carried out. The COP is measured about 0.49. Liu et al. [14] developed a new adsorption water chiller without refrigerant valves. The working pair is silica gel-water with mass recovery process. The COP range was 0.2-0.42 depending on the operating conditions.

Saha et al. [15] proposed a new two-stage non-regenerative adsorption chiller design and experimental prototype silica gel-water adsorption chiller. To exploit solar/waste heat of temperatures below 70°C, staged regeneration is necessary. The two-stage cycle can be

operated effectively with 55°C solar/waste heat in combination with a 30°C coolant temperature. He et al. [16] carried out a novel two stages adsorption chiller with different adsorbents such as Zeolite and activated carbon. The two-stage cycle can be operated effectively with a generator temperature of 45-50°C.

A two stage activated carbon cycle using R134a and R507A refrigerants in the two stages was investigated by Habib et al. [17]. The evaporator of the R134a cycle was connected to the condenser of the R507a system. The performance in this cycle was comparatively low, achieving COPs of only 0.04-0.1.

A novel three-bed, two-evaporator system was proposed and modeled by Miyazaki et al. [18]. The dual evaporator allows two beds to be adsorbing simultaneously, while a third is desorbing. A bed is connected to a low pressure evaporator and then when reaching near saturation conditions for that bed, it is connected to a high pressure evaporator and adsorption continues. COP for this system design increased by 70%, while SCP increased by 50% for this system design compared to a standard adsorption chiller working at the same conditions.

Several configurations were investigated by Li et al. [19], including a bed-to-bed re-adsorption process. It was found that using a bed-to-bed system improved the cooling capacity of the system by delivering cooling at both the evaporator and first adsorbent bed, although at different cooling output temperatures. The bed-to-bed design was also made adaptable so that the process could incorporate internal heat recovery, depending on the desired output, or operate as a conventional system. The COP doubled when operating in bed-to-bed mode compared to conventional operation.

K. Habib et al. [20] presents the theoretical analysis of the performance of solar powered combined adsorption refrigeration cycles that has been designed for Singapore and Malaysia and similar tropical regions using evacuated tube solar collectors. This novel cycle amalgamates the activated carbon (AC)-R507A as the bottoming cycle and activated carbon-R134a cycle as the topping cycle and deliver refrigeration load as low as -10 °C at the bottoming cycle. A simulation program has been developed for modeling and performance evaluation for the solar driven combined adsorption refrigeration cycle using the meteorological data of Singapore and Malaysia. The results show that the combined cycle is in phase with the weather. The optimum cooling capacity, coefficient of performance (COP) and chiller efficiency are calculated in terms of cycle time, switching time, regeneration and brine inlet temperatures.

A. Sadeghlu et al. [21], divided combined ADRS into four types based on different arrangements of two working pairs, Zeolite 13x/CaCl<sub>2</sub>-water and Silica gel (RD type)-water, to analyze the performance of combined ADRS. After validating mathematical models

with available experimental data, ADRS is simulated by using Simulink–Matlab software to achieve optimum times for various processes. The results of simulation show that the cooling capacity of the system with Zeolite 13x/CaCl<sub>2</sub>-water is more than the other types. The results have shown that the arrangement of adsorbents affects cooling capacity of combined ADRS significantly. In Type A, Zeolite 13x/CaCl<sub>2</sub>-water has been used as an adsorbent for both top and bottom cycles. This type not only has more cooling capacity than the other types, but also the effect of hot water temperature on cooling capacity of this type is less than the others. Furthermore, a sensitivity analysis has been done to determine the importance of each parameter on ADRS system because the cooling capacity and the COP are influenced by many constant parameters.

The objective of this paper is the development of a global simulation model flexible in changing operating conditions using Simulink. The optimization tools are used to enable selecting the optimum operating conditions corresponding to the best performance in order to adapt this machine in to Tunisian climate that having a cooling temperature up to 40°C and heating temperature up to 85°C.

## II. EXPERIMENTAL DEVICE

Figure 1 illustrates the experimental unit, driven by solar energy, provided from solar collectors, and the fuel source such as the natural gas. This platform combine cogeneration (by the production of electricity and heating), solar cooling, and sustainable construction (wood structure). Two similar adjacent chambers, with opposite comfort demand, are the users of heating and refrigeration.

The major components contained in the platform and ENERBAT which are included in the experiments carried out are:

*Solar panel:* On the roof, a solar field with 16 solar collectors, 2.4 m<sup>2</sup> each is installed. The collector characteristics are given in the following:

*Hot water tank thermal stratification:* The heat provided by the solar panel or by the co-generator is stored in the hot water cylinder, to thermal lamination, with a capacity of 1500 liters. The hot water fed from the tank to the adsorption refrigerating machine.

*Dry cooler:* The dry cooler constitutes the cooling circuit of the machine adsorption

*Two-room climate:* it consists of two rooms a warm room and a hot room represents the test cell.

*Adsorption refrigerating machine:* The adsorption machine, SorTech brand, the product chilled water circulating through the cooling ceiling of the cold room. Hot water supplied from the refrigerating machine of the balloon.

**Co-generator:** The used co-generator is an internal combustion engine coupled with electric generator which recovers more than 90 % of heat from coolant, lubricant, and exhaust gas. Thus, it is used as mean of producing electricity (220 V, 50 Hz) and heat (hot water at 85°C). Its electrical and thermal efficiencies are approximately 25 % and 65 %, respectively.

**Data acquisition:** The data are acquired and manipulated as two dimensional graphs and tabulated. Instrumentation also allows regulation of the tri-generation unit.

In this paper we focus only on the refrigeration machine for which we developed a simulation model that is confronted to experimental measurements.

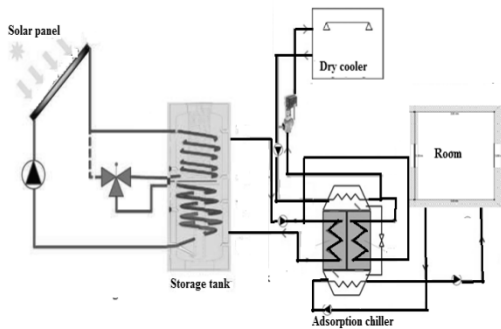


Fig. 1: Experimental device (Enerbat platform)

### III. MATHEMATICAL MODEL

#### a) Assumptions

In order to develop a mathematical model, a number of assumptions are required.

- ✓ The temperature, pressure and the amount of water vapor adsorbed are uniform throughout the adsorber beds.
- ✓ There is no external heat loss to the environment as all the beds are well-insulated.
- ✓ The condensate can flow into the evaporator easily.
- ✓ All desorbed water vapor from the desorber will flow into the condenser immediately and the condensate will flow into the evaporator directly.
- ✓ The condensate will evaporate instantaneously in the evaporator and will be adsorbed in the adsorber immediately.
- ✓ The adsorbed phase is considered as a liquid and the adsorbate gas is assumed to be an ideal gas.

#### c) Energy balance of adsorber

The adsorption energy balance is described by:

$$(m_{ad} c_{ad} + m_a c_a + m_a w c_{p,r}) \frac{dT_{ad}}{dt} = m_a \Delta H_{ads} \frac{dw}{dt} + m_a c_{p,r,v} \frac{dw}{dt} (T_{ev} - T_{ad}) + \dot{m}_{f,ad} c_{p,f} (T_{f,in} - T_{f,out}) \quad (6)$$

The outlet temperature of cooling water can be expressed as

$$T_{ad,out} = T_{ad} + (T_{ad,in} - T_{ad}) \exp \left( - \frac{U_{ad} A_{ad}}{\dot{m}_{f,ad} c_{p,f,ad}} \right) \quad (7)$$

- ✓ The thermal resistance between the metal tube and the adsorbent bed is neglected.
- ✓ Flow resistance arising from the water flowing in the pipeline is neglected.
- ✓ The properties of the fluid, the metal tube and adsorbate vapor are constant.

According to these assumptions, the dynamic behavior of heat and mass transfer inside different components of the adsorption chiller can be written as shown below.

#### b) Rate of Adsorption/desorption

The rate of adsorption or desorption is calculated by the linear driving force kinetic equation, The coefficients of LDF equation for silica gel/water are determined by Chihara and Suzuki [22] and are given in the below.:

$$\frac{\partial w}{\partial t} = K_s (w^* - w) \quad (\text{kg/kg.s}) \quad (1)$$

The effective mass transfer coefficient inside the pores  $k_s$  is given by:

$$K_s = F_0 \frac{D_s}{R_p^2} \quad (\text{s}^{-1}) \quad (2)$$

The effective diffusivity is defined as follows:

$$D_s = D_{s0} e^{-E_a/RT} \quad (\text{m}^2/\text{s}) \quad (3)$$

Where:

$$D_{s0} = 2.54 \cdot 10^{-4} \text{m}^2/\text{s}, R_p = 1.7 \cdot 10^{-4} \text{m}, E_a = 4.2 \cdot 10^4 \text{J/mol}, F_0 = 15$$

$$R = 8,314 \text{J/mol K}$$

The equilibrium uptake of silica gel- water pair is estimated using the equation developed by Boelman [23].

$$w^* = 0.346 \left( \frac{P_s(T_r)}{P_s(T_a)} \right)^{1/1.6} \quad (\text{kg}_{\text{water}}/\text{kg}_{\text{silica el}}) \quad (4)$$

Where  $P_s(T_w)$  and  $P_s(T_s)$  are respectively the corresponding saturated vapor pressures of the refrigerant at temperatures  $T_r$  (water vapor) and  $T_a$  (adsorbent).  $P_s$  for water vapor is estimated using the following equation:

$$P_{\text{sat}}(T) = 133,32 \exp \left( 18,3 - \frac{3820}{T-46,1} \right) \quad (5)$$

## d) Energy balance of desorber

The desorption energy balance is described by:

$$(m_{de} c_{de} + m_a c_a + m_a w c_{p,r}) \frac{dT_{de}}{dt} = m_a \Delta H_{ads} \frac{dw}{dt} + \dot{m}_{f,de} c_{p,f} (T_{f,in} - T_{f,out}) \quad (kW) \quad (8)$$

The outlet temperature of hot water can be expressed as

$$T_{de,out} = T_{de} + (T_{de,in} - T_{de}) \exp\left(-\frac{U_{de} A_{de}}{\dot{m}_{f,de} c_{p,f}}\right) \quad (9)$$

## e) Energy balance of condenser

The condenser energy balance equation can be written as

$$(m_{r,cd} c_{p,r} + m_{cd} c_{cd}) \frac{dT_{cd}}{dt} = -m_a \frac{dw_{des}}{dt} L_v - m_a c_{p,r,v} \frac{dw_{des}}{dt} (T_{de} - T_{cd}) + \dot{m}_{f,cd} c_{p,f} (T_{f,in} - T_{f,out}) \quad (kW) \quad (10)$$

The outlet temperature of cooling water can be expressed as

$$T_{cd,out} = T_{cd} + (T_{cd,in} - T_{cd}) \exp\left(-\frac{U_{cd} A_{cd}}{\dot{m}_{f,cd} c_{p,f,cd}}\right) \quad (11)$$

## f) Energy balance of evaporator

The energy balance in the evaporator is expressed as

$$(m_{ev} c_{ev} + m_{r,ev} c_{p,r}) \frac{dT_{ev}}{dt} = -m_a \frac{dw_{ads}}{dt} L_v - m_a \frac{dw_{des}}{dt} c_{p,r} (T_{cd} - T_{ev}) + \dot{m}_{f,ev} c_{p,f} (T_{f,in} - T_{f,out}) \quad (kW) \quad (12)$$

The outlet temperature of chilled water can be written as

$$T_{ev,out} = T_{ev} + (T_{ev,in} - T_{ev}) \exp\left(-\frac{U_{ev} A_{ev}}{\dot{m}_{f,ev} c_{p,f,ev}}\right) \quad (13)$$

## g) Mass balance in the evaporator

The mass balance for the refrigerant can be expressed by neglecting the gas phase as:

$$\frac{dm_{r,ev}}{dt} = -m_a \left( \frac{dw_{ads}}{dt} + \frac{dw_{des}}{dt} \right) \quad (14)$$

Where,  $m_a$  is the adsorbent mass.

## h) System performance equations

The COP value is defined by the following equation:

$$COP = \frac{Q_{ev}}{Q_{de}} \quad (15)$$

The cooling capacity of the system is expressed by:

$$Q_{ev} = \frac{\int_0^{t_{cycle}} \dot{m}_{f,ev} c_{p,f} (T_{ev,in} - T_{ev,out}) dt}{t_{cycle}} \quad (16)$$

Where:

$$Q_{de} = \frac{\int_0^{t_{cycle}} \dot{m}_{f,de} c_{p,f} (T_{de,in} - T_{de,out}) dt}{t_{cycle}} \quad (17)$$

Specific Cooling Power

$$SCP = \frac{Q_{ev}}{m_a} \quad (18)$$

Where:

$$m_a = 50 \text{ Kg}, \Delta H_{ads} = 2800 \text{ kJ/kg}, L_v = 2500 \text{ kJ/kg}, C_{cd}, C_{ev}, C_{ad} = 0.386 \text{ kJ/kg.K}, C_{p,r,v} = 1.85 \text{ kJ/kg.K}, \\ C_a = 0.924 \text{ kJ/kg.K}, C_{p,r} = 4.18 \text{ kJ/kg.k}, \dot{m}_{f,ad} = 1.6 \text{ m}^3/\text{h}, \dot{m}_{f,cd} = 3.7 \text{ m}^3/\text{h}, \dot{m}_{f,ev} = 2 \\ \text{m}^3/\text{h}, T_{ev,in} = 15^\circ\text{C}, T_{cd,in} = 22^\circ\text{C}, T_{gn,in} = 62^\circ\text{C}, t_{cycle} = 840 \text{ s},$$



### IV. RESULTS AND DISCUSSION

#### a) Model validation

Figure 2 shows the experimental and numerical temperature profiles of the hot, cooling and chilled water. After about 7mn, the hot water outlet temperature approaches to the inlet temperature, thus the heat consumed by the desorber after this point, will be quite small. But the difference between outlet and inlet temperature for the cooling water 1.8°C after cooling the adsorber for 7mn which shows that adsorber is sufficiently cooled down and the adsorption ability remains strong until the end of adsorption phase. Therefore the cycle time is taken as 14mn. It is worthy of note that the difference between outlet and inlet temperature of hot water after heating the desorber for 7mn is 3°C. It is also observed that the outlet temperature of chilled water reaches its minimum after each bed is heated/cooled for 50s. At this point the cooling power is at its maximum and the outlet temperature of chilled water is 11.8°C. The switching time is taken as 40s.

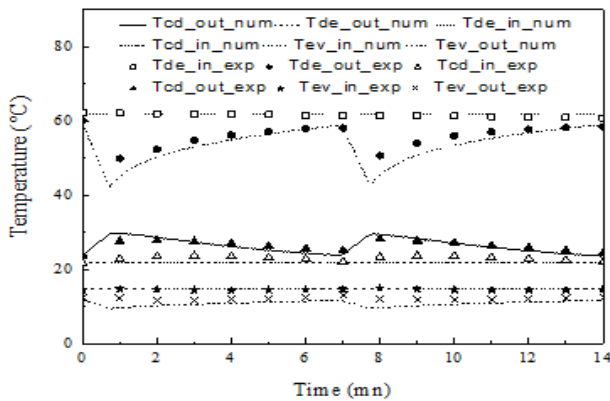


Fig. 2: Overall outlet temperature profile of heat transfer fluid for two beds adsorption chiller.

#### b) Parametric Study of the adsorption machine

Cooling / Heating/chilled water inlet temperature influences adsorption chiller performance. Lowering cooling water inlet temperature not only increases cooling capacity, but also enhances adsorption chiller COP, due to the significant increase in adsorption rate. Increasing heating water temperature also enhances chiller cooling capacity due to enhancing desorption rate that generate the adsorbed refrigerant prior to the evaporation/adsorption mode. However, it negatively influences the chiller COP depending on the cooling water inlet temperature.

- Effect of hot water inlet temperature

Figure 3 presents the change in chiller cooling capacity (SCP) and COP versus hot water inlet temperature at various cooling water inlet temperatures. Other operating conditions (cycle time, chilled water inlet temperature and secondary fluid flow rate) remain

constant at their design values. As the hot water inlet temperature increases the chiller cooling capacity increases for all cooling water inlet temperatures. As for COP, with hot water temperature variation from 55 to 95 °C, COP increases. Because a higher hot water temperature causes a higher heating power as well as a higher refrigerating capacity. For temperatures below 85°C, remained relatively constant with the increase in the generation temperature, this is due to the insufficient refrigerant circulation required to generate the cooling power.

It is clear that the sorption process is much faster for the highest temperatures. This means that the increase of hot water inlet temperature allows an increase in the rate of desorption and thereafter a faster heat transfer that generates the refrigerant adsorbed before the evaporation / adsorption phase.

Lowering the cooling water temperature increases the specific cooling capacity and coefficient of performance, because the condensation is faster for lower condenser cooling water temperatures, also because of the increase in adsorption rate.

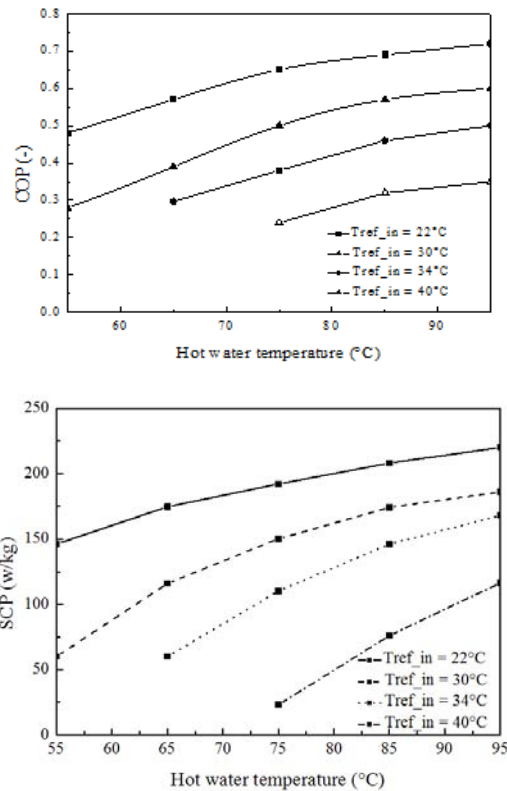


Fig. 3: Hot water inlet temperature influence on chiller COP and SCP (Tev\_in=15°C, tcycle=840s).

Figure 4 shows the change in the outlet chilled temperature versus hot water inlet temperature for variable cooling water inlet temperature, there is a slight variation of the evaporator outlet temperature that decreases with an increasing the heating water temperature.

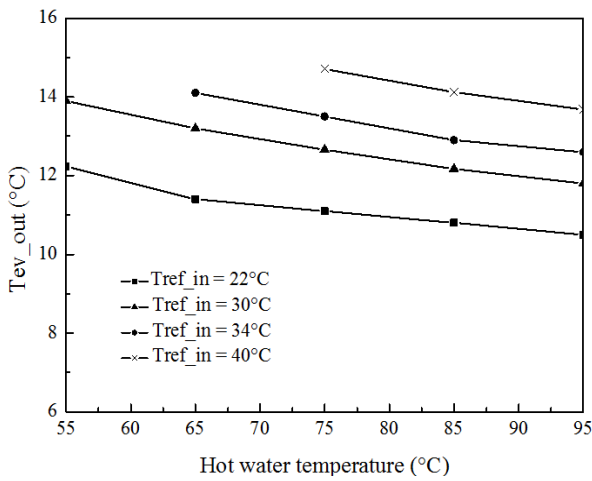


Fig. 4: Hot water inlet temperature influence on  $T_{ev\_out}$  ( $T_{ev\_in}=15^{\circ}\text{C}$ ,  $t_{cycle}=840\text{s}$ ).

The efficiency shows the ratio between the actual coefficient of performance and the Carnot cycle coefficient of performance ideal inverse (Figure 5).

The Carnot coefficient of performance is calculated by the following relation:

$$COP_{carnot} = \left[ \frac{T_{ad} - T_{de}}{T_{de}} \right] * \left[ \frac{T_{ev}}{T_{ad} - T_{ev}} \right] \quad (19)$$

The adsorption efficiency of the machine is determined by:

$$\eta = \frac{COP}{COP_{carnot}} \quad (20)$$

Efficiency increases with increasing hot water inlet temperature and lowering the cooling water inlet temperature.

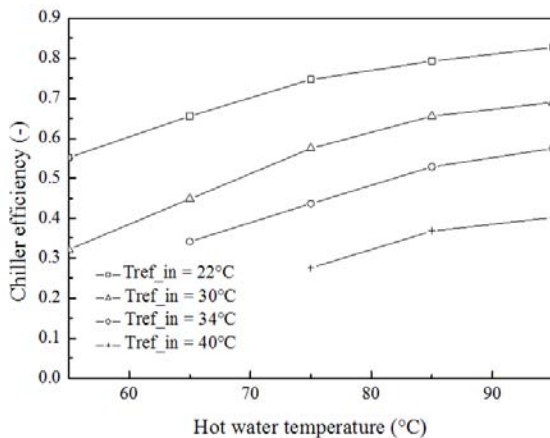


Fig. 5: Hot water inlet temperature influence on chiller efficiency ( $T_{ev\_in}=15^{\circ}\text{C}$ ,  $t_{cycle}=840\text{s}$ ).

• Effect of chilled water inlet temperature

In this part, the hot water inlet temperature is set at  $85^{\circ}\text{C}$  and the cooling water inlet temperature is  $40^{\circ}\text{C}$  (as Tunisian conditions), we will vary the chilled water inlet temperature and see the effect on the performance of the adsorption chiller.

Figure 6 shows the change in COP and SCP versus the inlet evaporator temperature, it is noted that for a variation of the latter to  $20^{\circ}\text{C}$  a variation of COP and SCP respectively  $0.2$  and  $0.481\text{ kW / kg}$ ; thus increasing the evaporator inlet temperature increases evaporation rates and then increase the cold production thus increasing system performance.

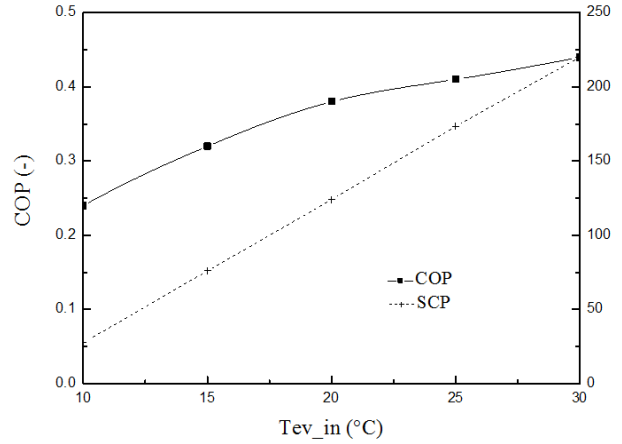


Fig. 6: Effect of chilled water inlet temperature on COP and SCP ( $T_{ref\_in}=40^{\circ}\text{C}$ ,  $T_{de\_in}=85^{\circ}\text{C}$ ,  $t_{cycle}=840\text{s}$ ).

Figure 7 shows the chilled water outlet temperature against its inlet temperature. It is found that the temperature difference between inlet and outlet are kept in constant, which means they are in linear relationship, for an inlet chilled water temperature of  $30^{\circ}\text{C}$  we can have a chilled outlet temperature of  $27^{\circ}\text{C}$ .

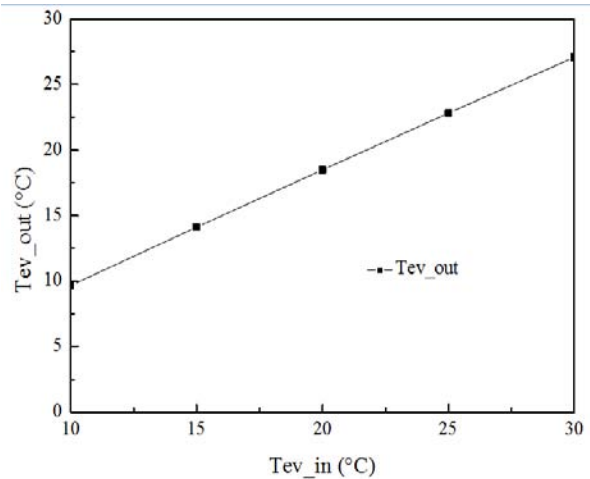


Fig. 7: The relationship between chilled water outlet temperature and inlet temperature. ( $T_{ref\_in}=40^{\circ}\text{C}$ ,  $T_{de\_in}=85^{\circ}\text{C}$ ,  $t_{cycle}=840\text{s}$ ).

• Effect of cycle time

The refrigeration capacity and COP variations with the cycle time are shown in Figure 8, the Operating conditions are setting in table 1. The COP increases uniformly with extension of the cycle time under a driving heat source of  $85^{\circ}\text{C}$ . This is because a longer cycle time causes much lower consumption of driving heat, the

maximum COP can be obtained at maximum adsorption / desorption time, which correspond to the minimum heating capacity and maximum adsorbed refrigerant amount. Based on the aforementioned results, the aim

is to have a short cycle time with a reasonable performance, so the optimal time 1240s cycle can be a tool to optimize adsorption system.

Table 1: Operating conditions

Tde_in	Tref_in	TeV_in	Total cycle time
85 °C	40 °C	15 °C	640-1400 s
Pre-heating/cooling time	Hot water flow rate	Cooling water flow rate	Chilled water flow rate
40 s	1.6 m3/h	3.7 m3/h	2 m3/h

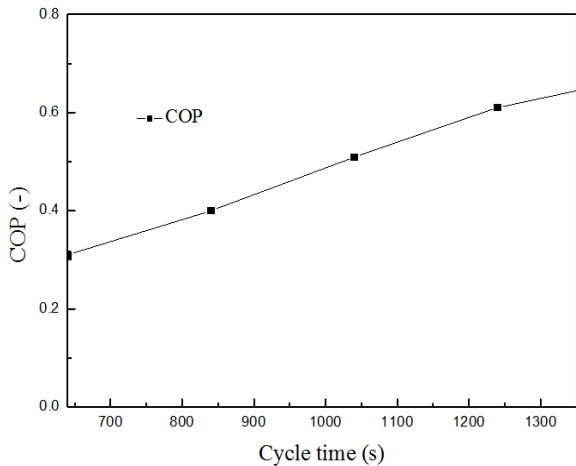


Fig. 8: Effect of cycle time on the COP (Tde\_in=85°C, Tref\_in=40°C, Tev\_in=15°C).

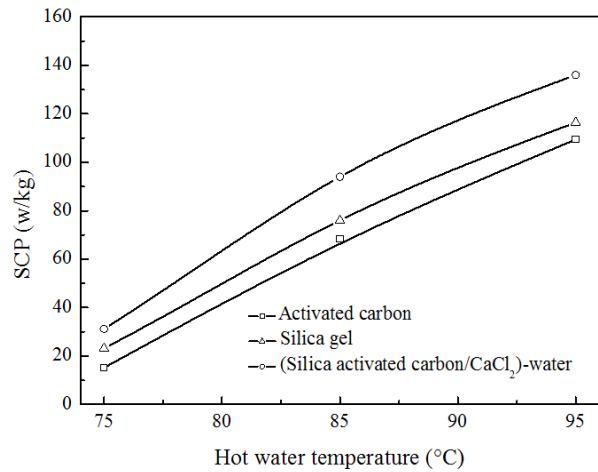
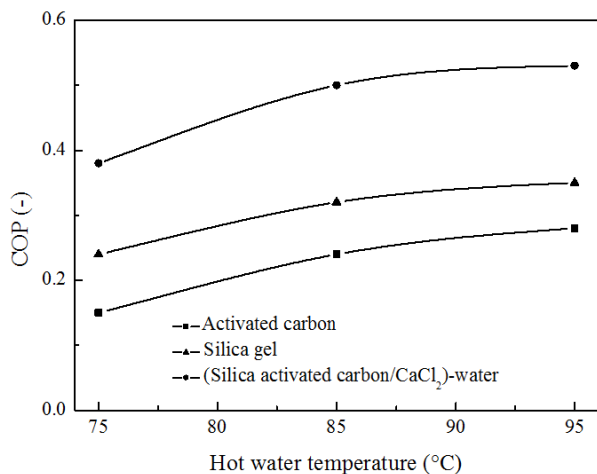


Fig. 9: Hot water inlet temperature influence on chiller COP and SCP (Tcycle=840s, Tref\_in=40°C, Tev\_in=15°C).

Figures 9 present the variation of COP and SCP according to the hot water inlet temperature. Indeed, water vapor is desorbed rapidly to a higher regeneration temperature to desorb most of the water vapor to be adsorbed in the next adsorption process.

Curves COP and the SCP for different adsorbents; silica gel, activated carbon and adsorbent composite (silica activated carbon/CaCl<sub>2</sub>)/eau, shows that for adsorbent composite, the COP and SCP is greater.



V. CONCLUSION

This work presents a solar adsorption refrigeration system using silica gel / water pairs. We have developed a numerical model for simulating the heat and mass transfer of the adsorption and regeneration processes in the two beds. This allowed us to study the influence of the regeneration, cooling and evaporator inlet temperature on the performance of the machine. The results show that the study parameters have a great impact on system performance for its adaptation to the Tunisian climate. It is preferable to work with a high regeneration and evaporation temperature where the coefficient of performance reaches its maximum value and a lower temperature at the cooling water of condenser and adsorber. The adaptation of chiller to the Tunisian climate was made. for a hot water inlet temperature of 85°C and a cooling water inlet temperature of 40°C we had a COP=0,3 and an SCP= 57 W/kg.

REFERENCES RÉFÉRENCES REFERENCIAS

1. Ghilen. N; Gabsi. S; Messai. S; Benelmir. R; El Ganaoui. M; 2016 Performance of silica gel-water solar adsorption cooling system. Case Studies in Thermal Engineering, 8, 337–345.



2. Benelmir. R; Ghilen. N; El Ganaoui. M; Deuscieux. D; S. Gabsi, 2013 Technology Platform ENERBAT - Gas Cogeneration, Solar Heating and Cooling: Int. J. of Thermal & Environmental Engineering, 4, 79 - 85.
3. Ghilen. N, Descieux; D, benelmir. R, 2014 Plateforme Technologique ENERBAT Cogénération - Froid solaire par adsorption – Construction Bois, SOCIETE FRANCAISE DE THERMIQUE, Groupe « Thermodynamique » Journée thématique, Problématiques Scientifiques et Technologiques dans les Procédés Frigorifiques et Thermiques à Sorption.
4. E.C. Boelman, B.B. Saha, T. Kashiwagi, 1995 Experimental investigation of a silica gel–water adsorption refrigeration cycle—the influence of operating conditions on cooling output and COP, ASHRAE Trans 101 (Part 2) 358–366.
5. Chi Yan Tso, Sau Chung Fu, Christopher Y.H. Chao., 2014 Modeling a solar-powered double bed novel composite adsorbent (silica activated carbon/CaCl<sub>2</sub>)–water adsorption chiller, BUILD SIMUL.
6. Tso, C. Y., C. Y. H. Chao and S. C. Fu, 2012 Performance Analysis of a Waste Heat Driven Activated Carbon Based Composite Adsorbent – Water Adsorption Chiller Using Simulation Model, International Journal of Heat and Mass Transfer.
7. Sapienza, A., S. Santamaria, A. Frazzica and A. Freni, 2011 Influence of the Management Strategy and Operating Conditions on the Performance of an Adsorption Chiller, Energy, 36, 5532-5538.
8. G. Restuccia, A. Freni, S. Vasta, Yu. Aristov,, 2004 Selective water sorbent for solid sorption chiller: experimental results and modeling, Int J Refrigeration; 27284–27293.
9. Y. L. Liu, R. Z. Wang, and Z. Z. Xia, 2005 “Experimental performance of a silica gel-water adsorption chiller,” Applied Thermal Engineering, vol. 25, no. 2-3, pp. 359–375,
10. Tomas Núñez,, Walter Mittelbach, Hans-Martin Henning, 2007 Development of an adsorption chiller and heat pump for domestic heating and air-conditioning applications, Applied Thermal Engineering, 27, 2205-2212.
11. Wang DC, Wu JY, Xia ZZ, et al., 2005 Study of a novel silica gel-water adsorption chiller: part I. Design and performance prediction. Int J Refrig; 28(7): 1073–83.
12. Zaizhong Xia ,, Dechang Wang , Jincui Zhang,, 2008 Experimental study on improved two-bed silica gel–water adsorption chiller, Energy conversion & Management, 49 1469-1479.
13. C.J. Chen, R.Z. Wang\*, Z.Z. Xia, J.K. Kiplagat, Z.S. Lu., 2010 Study on a compact silica gel–water adsorption chiller without vacuum valves: Design and experimental study, Applied Energy, 87 2673-2681.
14. Y.L. Liu, R.Z. Wang, Z.Z. Xia., 2005 Experimental study on a continuous adsorption water chiller with novel design, International Journal of Refrigeration, 28, 218-230.
15. B.B. Saha, A. Akisawa, T. Kashiwagi,, 2001 Solar/waste heat driven two-stage adsorption chiller: the prototype, Renewable Energy 23, 93–101
16. Z. H. He, H.Y. Huang , L.S. Deng , H.R. Yuan, N. Kobayashi, M. Kubota ,Huhetaoli, D.D. Zhao., 2014 Development of novel type of two-stage adsorption chiller with different adsorbents, The 6th International Conference on Applied Energy – ICAE2014,
17. Habib, K., B. B. Saha, A. Chakraborty, S. Koyama and K. Srinivasan, 2011 Performance Evaluation of Combined Adsorption Refrigeration Cycles, International Journal of Refrigeration, 34, 129-137.
18. Miyazaki, T., A. Akisawa and B. B. Saha, 2010 The Performance Analysis of a Novel Dual Evaporator Type Three-Bed Adsorption Chiller, International Journal of Refrigeration, 33, 276-285.
19. Li, T. X., R. Z. Wang, J. K. Kiplagat and L. Ma, 2012 Performance Analysis of a Multi-Mode Thermochemical Sorption Refrigeration System for Solar-Powered Cooling, International Journal of Refrigeration ,35, 532-542.
20. K. Habib et al., 2013 Study on solar driven combined adsorption refrigeration cycles in tropical climate, Applied Thermal Engineering, 50,1582-1589
21. A. Sadeghlu et al., 2015 Simulation study of a combined adsorption refrigeration system, Applied Thermal Engineering, 87, 185-199
22. K. Chihara, M. Suzuki, 1983, Air drying by pressure swing adsorption. Journal of Chemical Engineering of Japan, Vol 16(4), pp. 293-298.
23. E.C. Boelman, B.B. Saha, and T. Kashiwagi, 1995, Computer simulation of a silica gel–water adsorption refrigeration cycle—the influence of operating conditions of cooling output and COP. ASHARE Transactions, pp. 348–355,

#### Nomenclature

A	Heat transfer area, m <sup>2</sup>
C <sub>p</sub>	Specific heat, kJ/kg.K
DSO	Coefficient, (m <sup>2</sup> /s)
E	Heat exchanger efficiency:
L	Latent heat of vaporization, kJ/kg
m	Masse, kg
m <sub>f</sub>	Mass flow rate, kg/s
ΔH	Isosteric heat of adsorption, kJ/kg
P	Pressure, Pa
Q	heat, kJ
SCP	Specific cooling power, kW/kg
t	Time, s

T	Temperatures, °C
U	Overall conductance, W/m <sup>2</sup> .K
w, w *	Instantaneous Uptake, Equilibrium uptake, kg de réfrigérant/kg d'adsorbant
COP	Coefficient of performance of the machine
Subscripts	
a	Adsorbent (silica gel)
ad	Adsorber
ads	Adsorption
cd	Condenser
cycle	Cycle
ev	Evaporator
de	Desorber
f	Coolant
in	Inlet
j	Coolant indice
max	Maximum
min	Minimum
num	Numerical
out	Outlet
r	Refrigerant
r,v	Refrigerant vapor
v	Vapor